

# GRNN: Generative Regression Neural Network - A Data Leakage Attack for Federated Learning

Hanchi Ren  
 Swansea University  
 United Kingdom  
 845231@swansea.ac.uk

Jingjing Deng  
 Swansea University  
 United Kingdom  
 j.deng@swansea.ac.uk

Xianghua Xie  
 Swansea University  
 United Kingdom  
 x.xie@swansea.ac.uk

## Abstract

*Data privacy has become an increasingly important issue in machine learning. Many approaches have been developed to tackle this issue, e.g., cryptography (Homomorphic Encryption, Differential Privacy, etc.) and collaborative training (Secure Multi-Party Computation, Distributed Learning and Federated Learning). These techniques have a particular focus on data encryption or secure local computation. They transfer the intermediate information to the third-party to compute the final result. Gradient exchanging is commonly considered to be a secure way of training a robust model collaboratively in deep learning. However, recent researches have demonstrated that sensitive information can be recovered from the shared gradient. Generative Adversarial Networks (GAN), in particular, have shown to be effective in recovering those information. However, GAN based techniques require additional information, such as class labels which are generally unavailable for privacy persevered learning. In this paper, we show that, in Federated Learning (FL) system, image-based privacy data can be easily recovered in full from the shared gradient only via our proposed Generative Regression Neural Network (GRNN). We formulate the attack to be a regression problem and optimise two branches of the generative model by minimising the distance between gradients. We evaluate our method on several image classification tasks. The results illustrate that our proposed GRNN outperforms state-of-the-art methods with better stability, stronger robustness, and higher accuracy. It also has no convergence requirement to the global FL model. Moreover, we demonstrate information leakage using face re-identification. Some defense strategies are also discussed in this work.*

## 1. Introduction

More often than not, the success of Deep Learning (DL) [37, 25, 33] relies on the availability of a large quan-

ity of data. A distributed learning is commonly used to speedup training on a large-scale dataset or to utilise multiple data sources in order to enhance model performance, and it typically contains a number of computing clients and a central server to aggregate the model [54, 70, 14, 13, 21, 40, 61, 48, 31, 41]. However, such distributed learning approaches may not be possible as they require centralised data for model training, due to data protection and data-privacy requirements. For instance, data providers (e.g., hospital, finance company, or government agent) are not willing to share their private data with algorithm providers, which causes the so-called “Data Islands” issue. Therefore, decentralised data-training approaches are more attractive since they are more likely to meet those requirements.

Federated Learning (FL) [42, 19, 63, 12, 60] was proposed to train a learning model without accessing the private training data on the data provider by only exposing the gradient information of the shared global model to the server. The gradient is generally considered as privacy-preserved and secure to be shared with the server. However, recent studies reported that the gradient-sharing scheme is in fact not secure [16, 59, 28, 44]. For example, the presence of a specific property of the training dataset can be identified [44]. Hitaj *et al.* [28] showed the feasibility of generating images that are similar to training images given a class label using Generative Adversarial Network (GAN) [22]. Zhu *et al.* [69] proposed a method namely Deep Leakage from Gradients (DLG) to recover original training data via updating the inputs instead of model parameters to approximate the gradient information. DLG is often criticised as it is unstable and sensitive to the size of the training batch (cf. Section 4). Furthermore, Zhao *et al.* [67] proposed Improved DLG (iDLG) that improves the success rate of DLG by only approximating the gradient of the last layer of the model. However, it only works with a batch size of 1 and struggles to generate meaningful data when the variation of the training dataset is large.

In this paper, we propose a novel data leakage attack

method, namely Generative Regression Neural Network (GRNN) to recover private training data from the shared gradient between the local client and the central server. The method is particularly suitable for FL systems as the required gradient and global model are readily available in this scenario. GRNN consists of two branches for generating fake training data and their corresponding labels. The model is then jointly trained in an end-to-end fashion by approximating the fake gradient calculated by the generated data and labels to the true gradient on the same global FL model. We empirically evaluate the feasibility of our method on several image classification tasks, and comprehensive comparison studies are carried out against DLG. The experimental results show that it is capable of recovering both data and their corresponding labels. The proposed method is significantly more stable when a large batch size is used and outperforms the state-of-the-art in terms of quality of recovered data and accuracy of label inference. The contributions of this work are fivefold:

- We propose a novel data leakage attack method for FL, which is capable of recovering private training data as well as their corresponding labels from the shared gradient.
- Comprehensive experiments are carried out, qualitative and quantitative results are presented to prove the effectiveness of GRNN. We also compare the proposed method against the state-of-the-art method, which shows that GRNN is superior in terms of the quality of recovered data and the accuracy of label inference. In addition, our method is much more stable than others with respect to the size of the training batch.
- We conduct a face re-identification experiment, and the quantitative result shows that using the image generated by proposed GRNN achieves higher *Top-1*, *Top-3* and *Top-5* accuracies compared to the state-of-the-art.
- We discuss the potential defense strategies and quantitatively evaluate the effectiveness of our method against Differential Privacy (DP) defense strategy.
- The implementation of the method is publicly available to ensure its reproducibility.

The rest of the paper is organised as follows: An overview of related works on data leakage attack are presented in Section 2. The proposed method is described in Section 3. The details of experiments, results, and defense strategies are provided in Section 4. Section 5 concludes the paper.

## 2. Related Work

We categorise the attack methods into two groups: partial data leakage attack and full data leakage attack. For the

former, we refer to those that can only reveal partial information from the training data, for example, to identify if one or many attributes are in the training data or recover the training images based on a blurred or masked images. For the latter, these methods can generate data that is similar to or the same as the training data from random values.

### 2.1. Partial Data Leakage Attack

To the best of our knowledge, [5] is the earliest work that targets privacy information leakage of Machine Learning (ML) model. In this paper, the authors build a novel meta-classifier, which is used to attack other ML classifiers for revealing sensitive information from training data. Specifically, the method assumes having full access to a well-trained target model, and a particular attribute is pre-set to be identified if it is in the training data or not. They first build up many synthetic training datasets which partially contain the pre-set attributes and the rest does not. Several classification models are then trained on the synthetic datasets. The architecture of these classification models is the same as the target model. Then, they treat the parameters in the classification models as the input to the meta-classifier for training. Finally, the parameters from the well-trained target model are fed into the meta-classifier model to identify if the particular attribute is in the training data. The target model and the meta-classifier model are both ML models, *e.g.*, Artificial Neural Network (ANN), Hidden Markov Model (HMM) [6], Support Vector Machine (SVM) [8] or Decision Tree (DT). The authors provide two examples in terms of evaluating their method. One is to identify the speaker’s nationality over a speech recognition dataset from HMM. Later, they use SVM to set up a network traffic classifier to distinguish two kinds of traffic circumstances and the meta-classifier is to identify the type of traffic. Meta-classifiers are both DT in these two examples. The work is further improved by [59]. They propose a shadow training technique that can identify if any specific samples are in the training dataset.

In terms of recovering obfuscated images, [43] is the first work to the best of our knowledge. Such obfuscated images are readily available from data protection techniques (*e.g.*, blur, mask, corrupt, *etc.*) [11, 39]. In [43], the authors utilise DL model to recover obfuscated images in classification tasks. The adversary must have access to part of the original training data that are used to train the attack model. For that reason, this method is not suitable in most real cases. In a more recent work [66], they utilise a GAN, which is trained on public dataset, to recover missing sensitive regions in an image. However, they assume that the adversary has the access to the well-trained target model as discriminator. Different to these previous methods, our GRNN can recover images and labels in full only with access to the shared gradient and the shared classification model, which is a typical setup in a FL system.

## 2.2. Full Data Leakage Attack

For a long time, the gradient information is generally regarded as safe to share. Based on this, distributed learning has been widely used in real-world applications. However, more and more research works have proved that the gradient-sharing scheme is not safe to protect sensitive data. Recent works [17, 16] explored privacy-preserving research topic on a variety of face recognition models including softmax classifier, multi-layer perceptron, and stacked denoising auto-encoder. They formulated the attack as an optimisation problem: have access to the model and find a possible input that can maximise the output confidence with respect to the label of the image. The attacker requires two essential pieces of information: the label of the input image and access to the model which returns confidence values.

In a more recent work [28], the attack is conducted among a distributed learning system. All participants have a common view on the DL model and labels, and gradients will exchange between them. They formulate the attack behavior to be a generation process using GAN. First, each participant needs to train its local model on their own dataset for several iterations and achieve accuracy beyond a pre-set threshold. After that, the updated local model would be the discriminator. Fix the weights in the discriminator and train a generator by maximising the confidence of one specific class. As this method generates images from one class at a time, so the differential of images among one class should be small. That is to say, the success of this method needs to satisfy that samples among one class should be as similar as possible and ones between classes should not [44]. The method requires labels as a hint, whereas ours only uses gradient information. Moreover, their method requires the shared classification model to be trained to achieve a pre-set accuracy before it can be used as a discriminator. We have no such requirement and GRNN can be deployed at any stage of the training process. In all of our experiments, we conducted the attack just after the first iteration. Crucially, the fidelity of generated data is much higher for our proposed method. The images recovered using their method are only consistent with the data distribution but have not correspondence with the training dataset. In other words, the generated image cannot match back to the training data.

A more general method in terms of gradient leakage, DLG, is proposed recently in paper [69]. They formulate the problem to be a regression problem as following: The method first obtains the shared local gradient from a victim participant and randomly initialise a batch of “dummy” images and “dummy” labels; Then use the “dummy” data to conduct a normal forward-backward propagation and obtain “dummy” gradient; Finally, the method updates the “dummy” data by minimising the distance between the “dummy” gradient and shared local gradient. Among all the gradient leakage methods, DLG is the only one that achieves exact

pixel-wise level data revealing without any assistance information. It can conduct the attack on a batch of images, but label inference accuracy can be poor. In [67], the authors introduced iDLG that can identify labels more accurately by computing the derivative of cross-entropy loss over one-hot labels with respect to each class. They found that the derivative value regarding the ground-truth label drops in [-1, 0], and others lie in [0, 1]. In this way, it is possible to identify the correct label in a naive way, but the batch size can not be more than 1.

Besides deficiency in label inference, we found that DLG and iDLG struggle on some complex distributed datasets, especially when the class number is large. But our GRNN does not suffer from such problems (cf. Table 7 and 3). The similar part between GRNN and DLG, as well as iDLG, is that we both formulate the problem as a regression problem. However, GRNN utilises a generative model whose input is a randomly initialised sequence to recover the data and label, followed by comparing the fake gradient and shared gradient to update the generative model, whereas DLG and iDLG regress the fake data and fake labels directly from a pair of randomly initialised “dummy” data.

## 3. Proposed Method

We propose a data leakage attack for typical FL system, where only local gradients and global model are shared across different clients. Fig. 1 shows the deployment of the proposed GRNN in a FL system. GRNN is deployed on the server which aggregates local models to produce a global model given the gradients that are computed on individual clients using their private training data. The proposed GRNN is able to recover the data from the local gradients shared between clients and server, which can be used for malicious purposes, such as stealing private data or evaluating the privacy protection and data leakage of learning models. In this section, we will first introduce a neural network model based FL system in Section 3.1, then the proposed attacking method, namely GRNN in Section 3.2.

### 3.1. Federated Learning

FL is a distributed training scheme that consists of multiple clients and one parameter server. The training data are restrictively accessible by only the owner themselves and used to train the model locally at client nodes. Instead, the gradients of those models are exchanged between the clients and server to aggregate the global model. There are various global fusion methods (*e.g.*, Federated Stochastic Gradient Descent (FedSGD) [58], Federated Averaging (FedAvg) [42]) proposed to aggregate gradients that are calculated based on local models at client nodes. In this paper, we use the classic FedAvg method to train deep neural networks over multiple parties which is the the most widely used FL algorithm. It runs a number of steps of Stochastic

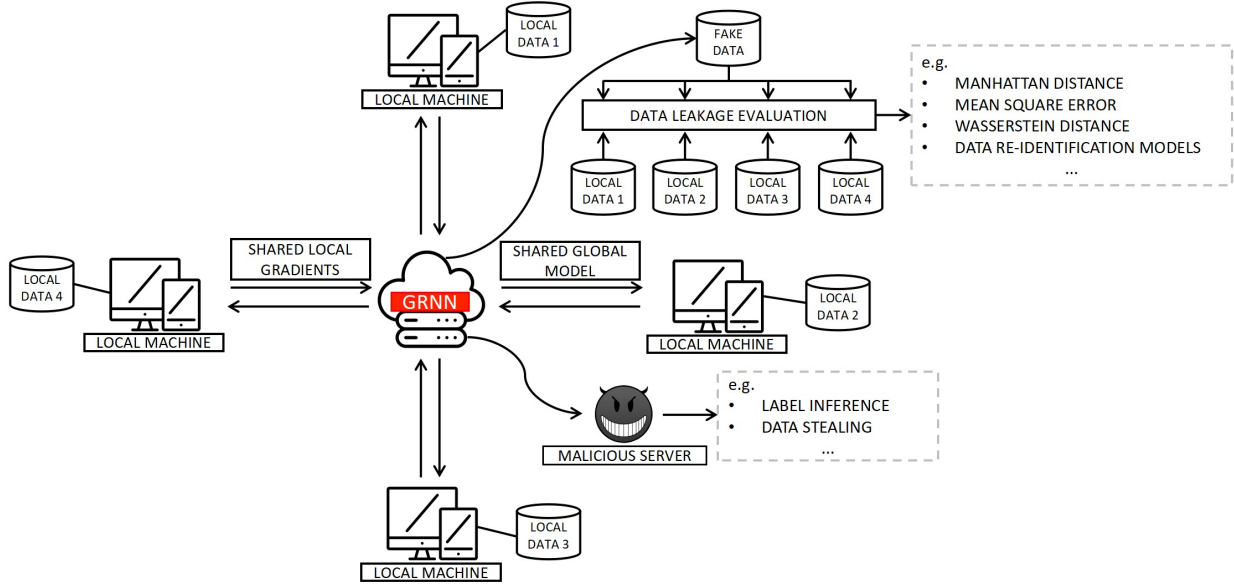


Figure 1. Illustration of how GRNN as a malicious server is deployed in a FL system.

Gradient Descent (SGD) in parallel on a small sampled subset of clients and then averages the resulting model updates via a central server periodically. The global model is merged by taking the average of gradients from local models according to  $\omega_t = \sum_i^N \frac{1}{N} \omega_i$ , where  $\omega_t$  and  $\omega_i$  are the gradients of global model and the  $i_{th}$  local model, and  $N$  is the total number of the clients.

We use a Convolutional Neural Network (CNN) based image classification model for learning in this paper, whereas FedAvg is applicable to any finite-sum objective. Formally, at iteration  $t$ , the  $i_{th}$  ( $i \in \{1, 2, \dots, C\}$ ) client computes its local gradient  $g_t^i$  based on local training data  $(x_t^i, y_t^i)$  and the parameterised learning model  $\theta_t$ , see Equ. 1, where  $F(\bullet)$ ,  $\theta_t$  and  $L(\bullet)$  are the global learning model, its network parameters at iteration  $t$  and loss function respectively. The local gradient  $g_t^i$  of learning model is calculated using typical SGD at each individual client node independently. The server aggregates the local gradient  $g_t^i$  and then updates the global model weights to  $\theta_{t+1}$ , as shown in Equ. 2 where  $C$  is the number of clients.

$$g_t^i = \frac{\partial L(F(x_t^i, y_t^i), \theta_t)}{\partial \theta_t} \quad (1)$$

$$\theta_{t+1} = \theta_t - \frac{1}{C} \sum_{i=1}^C g_t^i \quad (2)$$

### 3.2. GRNN: Data Leakage Attack

The proposed GRNN is deployed at the central server as illustrated in Fig. 1. We assume that the GRNN at the central server has access to the network architecture and

parameters of the global model. The only information that can be obtained between server and client is the gradient calculated based on the current global model that is distributed across all nodes given the private training data, where the gradient is normally considered as safe to share. To compute the gradient of the model, the private data, its corresponding label, and global model at current iteration are required at the local client. We hypothesise that the shared gradient contains the information of private data distribution and space partitioning given the global model. The architecture of GRNN shown in Fig. 2 has two branches that share the same input that is sampled from a common latent space. We consider that each point within this latent space represents a pair of image data and its corresponding label. The objective of the GRNN is to separate this tied representation in the latent space and recover the local image data and corresponding label by approximating the shared gradient that is accessible at the server node.

The top branch is used to recover image data, namely fake-data generator, which consists of a generative network model. The input random vector is first fed into a fractionally-strided convolutional layer [64, 65] to produce a set of feature maps with a resolution of  $4 * 4$ , which then go through several upsampling blocks that gradually increase the spatial resolution. The number of the upsampling block is determined by the resolution of the target image. For example, if the target image resolution is  $32 * 32$ , then 3 upsampling blocks ( $4 \rightarrow 8 \rightarrow 16 \rightarrow 32$ ) are used. In upsampling block, nearest-neighbour interpolation is used to recover the spatial resolution of feature maps from the previous layer. It

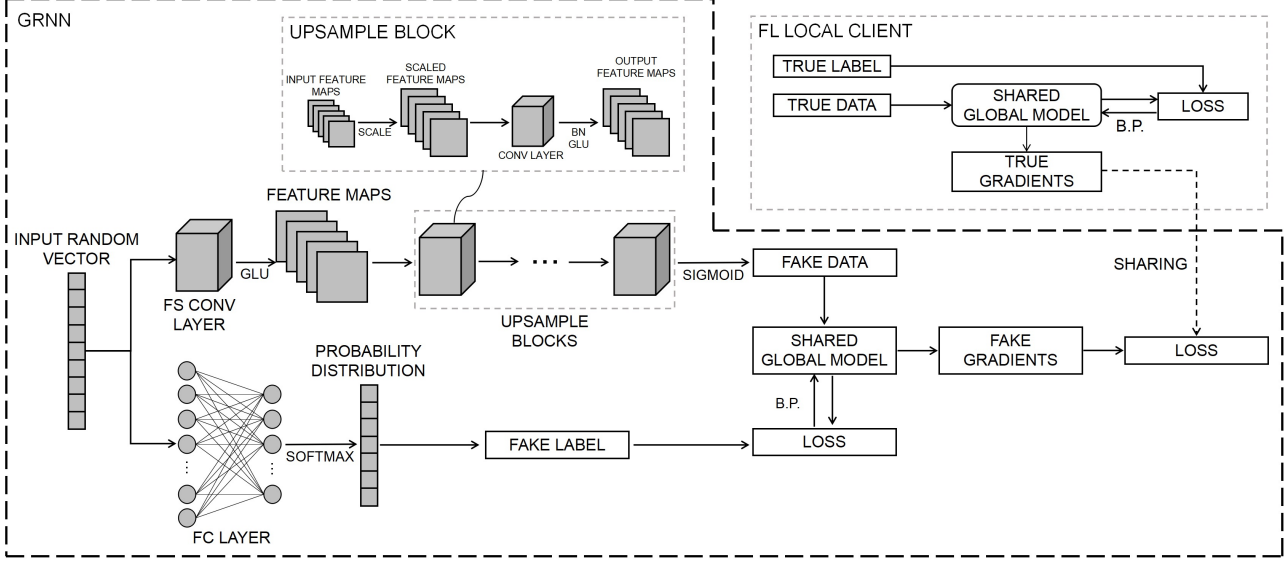


Figure 2. Details of the proposed GRNN where the top branch is for generating fake image and the bottom branch is for inferring the label. “FC LAYER” is fully-connected layer. “FS CONV LAYER” is fractionally-strided convolutional layer. Details of upsampling block, please refer to Table 1.

Table 1. Construction of upsampling block.

Layer Name	Setting
Upsampling Layer	scale factor: 2 mode: nearest
Convolutional Layer	kernel size: 3 stride: 1 padding: 1
Batch Normalization Layer	-
Gated Liner Unit	-

then passes through a standard convolutional sub-block that contains a convolutional layer, a batch normalisation layer, and a Gated Linear Unit (GLU) activation layer. The details of the upsampling block are listed in Table 1. At the end of the top branch, a data sample that has the same dimension as the training input of the federated learning system is generated, namely, fake-data. The bottom branch is used to recover label data, namely fake-label generator which contains a fully-connected layer followed by a softmax layer for classification. It takes a randomly sampled vector from latent space as input and outputs its corresponding label. We assume the elements in the input vector are independent of each other and subject to a standard Gaussian distribution. The label set in GRNN is identical to the one used in the federated learning system. Formally, the fake image data ( $\hat{x}_t^j$  and fake label  $\hat{y}_t^j$ ) generation can be formulated as in Equ. 3, where  $\hat{\theta}$  and  $v_t$  are trainable parameters of GRNN and input random vector sampled from a unit Gaussian distribution.

$$(\hat{x}_t^j, \hat{y}_t^j) = G(v_t | \hat{\theta}_t) \quad (3)$$

Given a pair of fake image and label that are generated as described above, a fake gradient on the current global model can be obtained via feeding them as training input and perform one iteration of SGD according to Equ. 1. The objective of GRNN is to approximate the true gradient using the fake image data and label generators, therefore, the whole model can be trained by minimising the distance between the fake gradient  $\hat{g}_t^j$  and shared true gradient  $g_t^j$ , i.e., the most commonly used loss Mean Square Error (MSE) is adopted here:

$$\begin{aligned} & \min_{\hat{\theta}} \|g_t^j - \hat{g}_t^j\|^2 \Rightarrow \\ & \min_{\hat{\theta}} \left\| \frac{\partial L(F(<\hat{x}_t^j, \hat{y}_t^j>, \theta_t))}{\partial \theta_t} - \frac{\partial L(F(<\hat{x}_t^j, \hat{y}_t^j>, \theta_t))}{\partial \theta_t} \right\|^2 \end{aligned}$$

Note that the gradient of the model is a vector, the length of which is equal to the number of trainable parameters. In addition to measuring discrepancy between the true and fake gradients based on Euclidean distance, we also introduce the Wasserstein Distance (WD) loss to minimise the geometric difference between two gradient vectors and Total Variation Loss (TVLoss) [56] to impose the smoothness constrain on generated fake image data. Therefore, the loss function for GRNN, namely  $\hat{L}(\bullet)$  is formulated as:

$$\hat{L}(g, \hat{g}, \hat{x}) = MSE(g, \hat{g}) + WD(g, \hat{g}) + \alpha \cdot TVLoss(\hat{x})$$

where we weight the MSE loss and WD equally and  $\alpha$  is the weighting parameter for smoothness regularisation. Both branches of the proposed GRNN are parameterised using a neural network that is completely differentiable and can be jointly trained in an end-to-end fashion. The complete training procedure for GRNN is described in Algorithm 1.

## 4. Experiment and Discussion

### 4.1. Dataset and Experimental Setting

A number of experiments on typical computer vision tasks including digit recognition, image classification, and face recognition were conducted to evaluate our proposed method. We used four public benchmarks, MNIST [36], CIFAR-100 [32], Labeled Faces in the Wild (LFW) [30] and VGG-Face [52] for those tasks. There are 7000 grey-scale handwritten digit images of  $28 \times 28$  resolution in the MNIST dataset. CIFAR-100 consists of 60000 color images of size  $32 \times 32$  with 100 categories. LFW is a human face dataset that has 13233 images from 5749 different people. We treated each individual as one class, hence, there are 5749 classes in total. VGG-Face consists of over 2.6 million human face images and 2622 identities. To keep the image resolution consistent across all experiments in this section, we resize all the images in LFW and VGG-Face datasets to  $32 \times 32$ .

*LeNet* [38] and *ResNet-18* [25] are used as the backbone networks for training image classifiers in FL system. All neural network models are implemented using PyTorch [53] framework and the source code has been made publicly available<sup>1</sup> for reproducing the results. In order to ensure the model to be second-order differentiable, *ReLU* activation layer is replaced with *Sigmoid* layer, where the model weights are randomly initialised. The batch size varies across different experiments, and a comprehensive comparison study was carried out. *RMSprop* optimiser with a learning rate of 0.0001 and a momentum of 0.99 is used for GRNN. Regarding the loss function of GRNN, we set the weights of TVLoss to  $1e - 3$  and  $1e - 6$  for *LeNet* and *ResNet-18*, respectively. Since our method has no requirement on the convergence of the shared global model and can be applied at any stage of the training period, we conducted the data leakage attack using GRNN after the first iteration of FL model aggregation. More implementation details related to specific experiments are presented in the corresponding sections.

### 4.2. Image Recovery

We first trained three CNN based image classifiers over one iteration on MNIST, CIFAR-100, and LFW datasets separately, and then used the proposed GRNN to conduct a data leakage attack on those models. Some qualitative results are presented in Table 2, where the middle column

shows the image data recovered from the true gradient that is shared between client and server. The images are recovered gradually with the number of iteration for training GRNN increases, while the true gradient is obtained only at the first iteration of global FL model, which indicates the gradient can lead to data leakage in FL regardless the convergence of shared global model.

A comparison study between the proposed GRNN and DLG was carried out using the same setting as described above, while we varied the training batch size of FL model to evaluate the feasibility of data leakage attack. It is reasonable to consider that the data recovery is more challenging when the training batch size is increasing as the shared gradient is averaged over all image data in the batch, where information of an individual image is obscurely mixed. Table 3 lists the success and failure of attack for both two methods. On MNIST dataset, DLG attack starts to fail when the size of training batch is larger than 8 and the *LeNet* is used in FL, whilst our method is able to recover the image data even with a batch size of 256. On CIFAR-100 and LFW datasets, DLG attack only works with a training batch size of 1, however, our method can still successfully perform the attack with a large batch size up to 64 and 128 respectively. Some failure examples of our method when a large training batch size is used can be found in Table 4. Although some failure examples show the consistency of color distribution and geometric similarity of objects, the appearance details are largely inconsistent or hard to match the original ones. We also show that the proposed GRNN can successfully attack complex and large models, such as *ResNet-18*.

To quantitatively evaluate the similarity of recovered images and true images, three metrics, namely MSE, WD and Peak Signal-to-Noise Ratio (PSNR) [29] are computed. Fig. 3 shows the MSE and WD between recovered images and true images with respect to training iteration of the attacking model. *LeNet* model as the global FL model was used in this experiment. The dash lines and the solid lines correspond to the results of DLG and GRNN, respectively. Although GRNN achieves slightly higher scores in MSE and WD when the batch size of 1 is used, our method is much more stable and significantly better when a larger batch size is used. When the batch size increases to 4 and 8, DLG only works on MNIST but fails on both CIFAR-100 and LFW, therefore, the corresponding similarity measurements can not converge (see the green and purple dashed lines in Figs. 3 (c) (d), (e) and (f)). DLG fails on all datasets with batch size of 16 while GRNN is able to recover the image data consistently (see Figs. 3 (g) and (h)). We also notice that DLG can well approximate the shared true gradient while generating a poor image. Fig. 4 shows that DLG achieves smaller MSE loss (Euclidean distance between true gradient and fake gradient) compared to our method, while it fails to recover the image data.

<sup>1</sup><https://github.com/Rand2AI/GRNN>

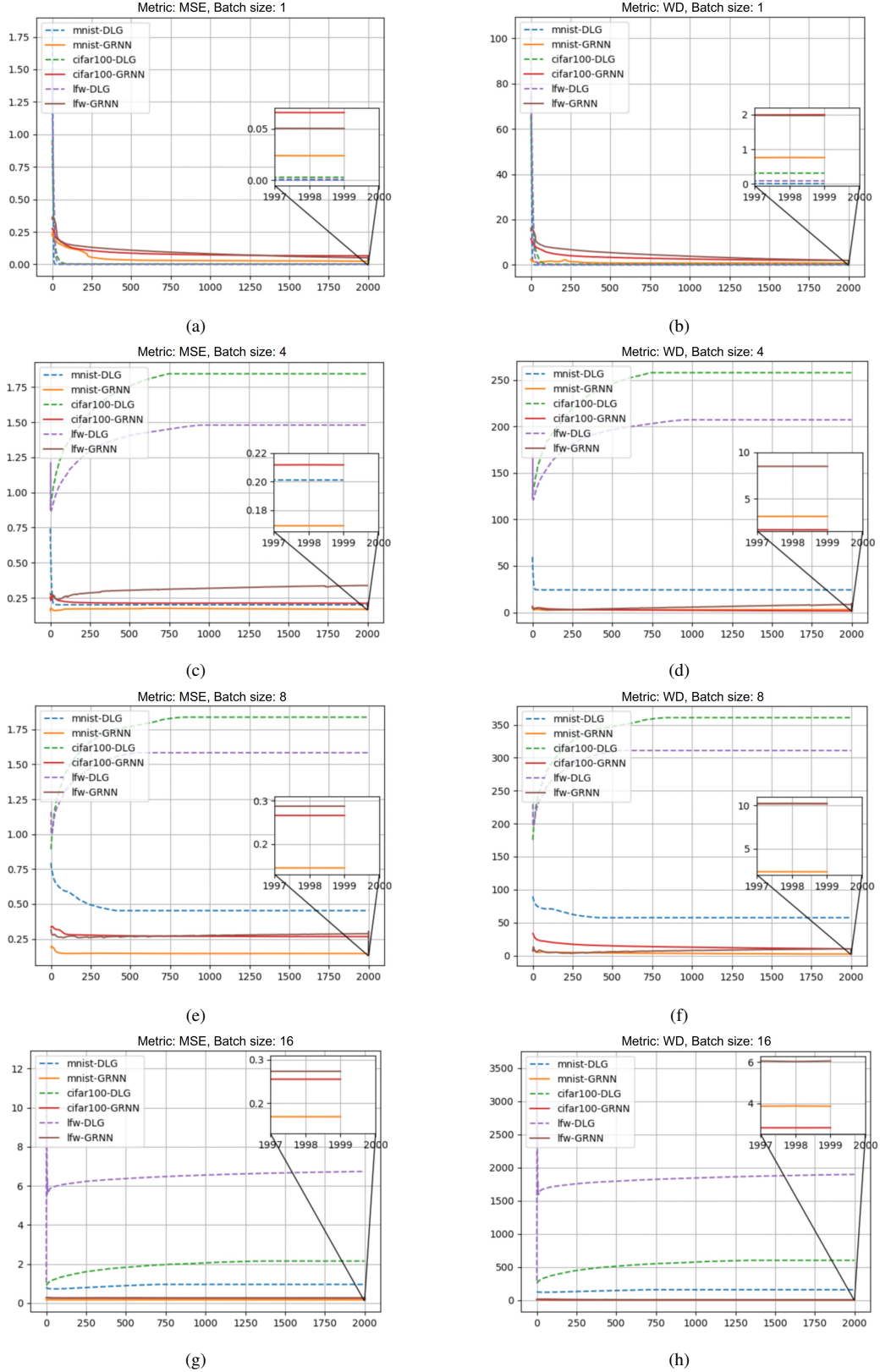


Figure 3. Distances between true and generated images with respect to training iteration for DLG and GRNN on three datasets. The horizontal axis corresponds to the number of training iterations of two attacking models and the vertical axis corresponds to the similarity metrics.

---

**Algorithm 1** GRNN: Data Leakage Attack

---

```

1:  $g_t^j \leftarrow \partial L(F(\langle x_t^j, y_t^j \rangle, \theta_t)) / \partial \theta_t$ ;           # Produce true gradient on local client.
2:  $v_t \leftarrow$  Sampling from  $\mathcal{N}(0, 1)$ ;                                     # initialise random vector inputs for GRNN.
3: for each iteration  $i \in [1, 2, \dots, I]$  do
4:    $(\hat{x}_{t,i}^j, \hat{y}_{t,i}^j) \leftarrow G(v_t | \hat{\theta}_i)$ ;                   # Generate fake images and labels.
5:    $\hat{g}_{t,i}^j \leftarrow \partial L(F(\langle \hat{x}_{t,i}^j, \hat{y}_{t,i}^j \rangle, \theta_t)) / \partial \theta_t$ ; # Calculate fake gradient on shared global model.
6:    $\mathcal{D}_i \leftarrow \hat{L}(g_t^j, \hat{g}_{t,i}^j, \hat{x}_{t,i}^j)$ ;                         # Calculate GRNN loss between true gradient and fake gradient.
7:    $\hat{\theta}_{i+1} \leftarrow \hat{\theta}_i - \eta (\partial \mathcal{D}_i / \partial \hat{\theta}_i)$ ;          # Update GRNN model.
8: end for
9: return  $(\hat{x}_{t,I}^j, \hat{y}_{t,I}^j)$ ;                                         # Return generated fake images and labels.

```

---

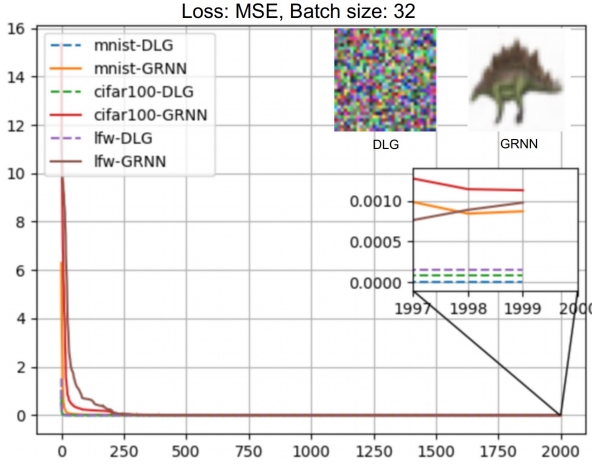


Figure 4. MSE loss visualisation for DLG and GRNN with batch size 32.

Although MSE and WD results from GRNN perform slightly worse than those from DLG with a batch size of 1, the difference between these two generated set of images at this batch size is hardly discernible. Hence, we further calculated PSNR to compare the pixel-wise similarity of the recovered images. PSNR is an objective standard for image evaluation which is defined as the logarithm of the ratio of the squared maximum value of RGB image fluctuation over MSE between two images, formally  $PSNR = 10 \cdot \lg(\frac{255^2}{MSE(img_1, img_2)})$ . The higher PSNR score, the higher the similarity between two images. Table 5 shows GRNN achieves higher PSNR on MNIST and LFW datasets (+1.45% and +0.52% respectively) and lower on CIFAR-100 dataset (-1.01%). Furthermore, our method achieved reasonable PSNR score on attacking *ResNet-18* model while DLG always fails. Table 6 shows some qualitative comparison of recovered images using both methods. We can observe that DLG recover the image pixel by pixel greedily, whereas GRNN also ensures the appearance distribution to be consistent with the true image in a coarser scale, and object details are then gradually filled at a finer scale.

### 4.3. Label Inference

In addition to image data recovery, we also investigated the performance of label inference in those experiments. Table 7 provides the comparative results of label inference accuracy (%) for DLG and GRNN, where each experiment was repeated 10 times, the mean and standard deviation were reported. We can observe that the label inference accuracy decreases while the size of the training batch increases for both DLG and GRNN. However, our method outperforms DLG in all experiments except the one on MNIST with a batch size of 8. Furthermore, GRNN is significantly better than DLG when large batch size is used. For example, GRNN achieves 99.84% on LFW using *LeNet* and a batch size of 256, whereas DLG only obtains 79.69% using the same setting. Note that having a correct label predicted does not necessarily indicate the corresponding image data can be recovered successfully (see Table 3). We can conclude that recovering image information is much more challenging than recovering label as the distribution of image data is in a much higher dimension than its corresponding label. The accuracy of label inference on *ResNet-18* achieved 100% in almost all experiments except the one on LFW with a batch size of 32 (94.06%), which is higher and more stable than *LeNet*. *ResNet-18* has much more trainable parameters than *LeNet*, therefore, the gradient with a larger number of elements is much more informative for finding decision boundaries for the classification task.

We also noticed that the number of label classes has an impact on its inference performance. In our experiment, MNIST, CIFAR-100, and LFW have 10 classes, 100 classes, and 5749 classes, respectively. The average accuracy of DLG is 94.23% on MNIST while decrease to 93.51% and 85.41% on CIFAR-100 and LFW, respectively. In contrast, GRNN achieved higher accuracy on LFW compared to the other two datasets. In DLG the label is obtained via updating the image input and label input jointly during the backward pass phase in SGD, whereas in GRNN the label is calculated by the fake label generator in the forward pass phase. We believe that by adding the image data and label generators,

Table 2. Examples of data leakage attack using the proposed GRNN.

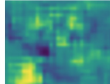
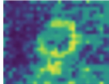
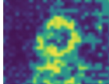
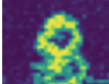
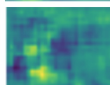
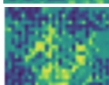
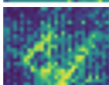
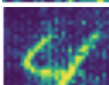
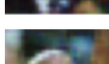
Dataset	Generated Data					True Data
MNIST						
						
CIFAR-100						
						
						
						
						
						
LFW						
						
						
						
						

Table 3. Data leakage attack with different sizes of training batch for FL model, where “✓” refers to a success and “✗” refers to a failure.

Method	Model	Dataset \ Batch	1	4	8	16	32	64	128	256
			MNIST	CIFAR-100	LFW					
DLG	LeNet	MNIST	✓	✓	✓	✗	✗	✗	✗	✗
		CIFAR-100	✓	✗	✗	✗	✗	✗	✗	✗
		LFW	✓	✗	✗	✗	✗	✗	✗	✗
	Ours	MNIST	✓	✓	✓	✓	✓	✓	✓	✓
		CIFAR-100	✓	✓	✓	✓	✓	✓	✓	✗
		LFW	✓	✓	✓	✓	✓	✓	✗	✗
Ours	ResNet-18	MNIST	✓	✓	✓	✓	✗	-	-	-
		CIFAR-100	✓	✓	✗	✗	✗	-	-	-
		LFW	✓	✗	✗	✗	✗	-	-	-

Table 4. Examples of failed data leakage attack using the proposed GRNN experiments on *LeNet* with batch size of 128 and 256. The top row shows the fake images recovered from the shared gradient and the bottom row shows corresponding images in the private datasets.



Table 5. PSNR scores achieved by DLG and GRNN with the batch size of 1.

Method	Model	Dataset	PSNR
DLG	LeNet	MNIST	50.90
		CIFAR-100	<b>48.59</b>
		LFW	45.05
Ours	LeNet	MNIST	<b>52.37</b>
		CIFAR-100	47.58
		LFW	<b>45.57</b>
	ResNet-18	MNIST	42.70
		CIFAR-100	38.85
		LFW	39.60

GRNN can better capture the correspondence between image data and its label in the joint latent space and, furthermore, can generate more individualised images with respect to different classes.

#### 4.4. Face Re-Identification

As shown in Table 6 recovered images look almost the same as their corresponding true images, there are still slight deviation which may produce classification misleading results if we use generated data to replace the original ones. This behaviour of deep learning methods are well documented in the literature, *e.g.*, [47, 51, 35, 45, 57]. Taking face recognition as an example, the recovered face image may look identical to its original image visually, however, it cannot produce correct prediction by the face recognition model to identify the person, see Table 9. Therefore, we

applied the face re-identification experiment to evaluate the feasibility of data leakage attack using GRNN. We first used the GRNN to recover the face image data from the FL system during the training. Then, the fake image was passed to the face recognition model as input to produce the identity label. A success of re-identification was counted if the prediction label matches the true label. The pipeline of the face re-identification experiment is shown in Fig. 5. VGG-Face dataset was used in this experiment which contains 2622 identities. We used the top 100 identities that have the most image samples for training. We selected the successfully recovered image data from the output of GRNN which ended up with 700 fake face images in total when batch size is 1, and 1112 images, 2224 images and 4352 images for batch size 4, 8, and 16 respectively. In the meantime, we trained two face recognition models using *ResNet-18* and *DenseNet-121* using the same training set. Table 8 reports the top-1, top-3 and top-5 accuracies of re-identification of those fake face images. Although the top-1 accuracy on *ResNet-18* and *DenseNet-121* are 30.66% and 11.46% when batch size is 1, they are significantly better than random prediction (1%). The re-identification accuracy increase dramatically when we consider using top-3 and top-5 metrics. The recovery performance becomes worse with the increasing of batch size, so the accuracy decreases as well. We say that the face recognition deep models are sensitive to the minor perturbation that is produced during the image recovery process. The images generated using GRNN achieve significantly higher accuracies compared to DLG, *i.e.*, +5.52%, +29.22% and

Table 6. Comparison of image recovery using DLG and GRNN.

True Data	DLG					GRNN				

Table 7. Comparison of label inference accuracy (%) using DLG and GRNN.

Method	Model	Dataset \ Batch Size	1	4	8	16	32	64	128	256	Avg
			100.0± 0.0	97.50± 0.0750	100.0± 0.0	94.38± 0.0337	90.62± 0.0242	90.31± 0.0260	91.41± 0.0152	92.42± 0.0181	94.23± 0.0254
DLG	LeNet	MNIST	100.0± 0.0	97.50± 0.0750	100.0± 0.0	94.38± 0.0337	90.62± 0.0242	90.31± 0.0260	91.41± 0.0152	92.42± 0.0181	94.23± 0.0254
		CIFAR-100	100.0± 0.0	97.50± 0.0750	98.75± 0.0375	97.50± 0.0306	92.50± 0.0287	89.84± 0.0329	86.33± 0.0295	85.70± 0.0289	93.51± 0.0329
		LFW	100.0± 0.0	80.00± 0.3317	90.00± 0.1561	85.00± 0.2358	88.44± 0.1683	70.62± 0.3924	89.53± 0.2985	79.69± 0.3985	85.41± 0.2477
Ours	LeNet	MNIST	100.0± 0.0	100.0± 0.0	97.50± 0.0500	97.50± 0.0415	97.50± 0.0187	96.25± <b>0.0188</b>	96.25± <b>0.0171</b>	96.37± <b>0.0165</b>	97.73± 0.0203
		CIFAR-100	100.0± 0.0	100.0± 0.0	100.0± 0.0	99.38± 0.0188	99.69± 0.0094	98.91± <b>0.0122</b>	98.75± <b>0.0080</b>	96.80± <b>0.0108</b>	99.19± 0.0074
		LFW	100.0± 0.0	97.50± 0.0750	98.75± 0.0375	100.0± 0.0	100.0± <b>0.0</b>	99.69± <b>0.0062</b>	99.69± <b>0.0071</b>	99.84± <b>0.0019</b>	99.43± <b>0.0160</b>
	ResNet-18	MNIST	100.0± 0.0	100.0± 0.0	100.0± 0.0	100.0± 0.0	100.0± 0.0	-	-	-	100.0± 0.0
		CIFAR-100	100.0± 0.0	100.0± 0.0	100.0± 0.0	100.0± 0.0	100.0± 0.0	-	-	-	100.0± 0.0
		LFW	100.0± 0.0	100.0± 0.0	100.0± 0.0	100.0± 0.0	94.06± 0.0452	-	-	-	98.81± 0.0090

+36.54% can be achieved in *Top-1*, *Top-3* and *Top-5* accuracies using *ResNet-121*.

#### 4.5. Defense Strategy

Recently, many studies have investigated privacy-preserving for sensitive data using cryptography in learning, such as secure aggregation protocol [7], Homomorphic Encryption (HE) [3, 20, 34], DP [15, 1, 55, 10] or linear regression [50, 18, 46], decision trees [4, 9], neural net-

works [20, 26, 49, 27, 34]. One possible defense strategy is to train the learning model in FL system using encrypted data. Our proposed GRNN should be capable of recovering the encrypted data from the shared gradient (as we make no assumption about the original data), although the original data is well protected without knowing the details of the encryption algorithm, *i.e.*, encryption keys. However, the cryptography operations are computationally expensive, and the consistency of visual patterns of images is generally not



Figure 5. The pipeline of the face re-identification experiment.

Table 8. Performances of different network architectures, where training accuracy refers to predicted results of true images and relevant ground truth. Re-identification accuracy is from predicted results of fake images and relevant ground truth. DLG and GRNN both use LeNet as backbone. Training and testing samples are from VGG-Face dataset.

Method	Network	Training Accuracy	Batch Size	Re-identification Accuracy			Sample Number
				Top-1	Top-3	Top-5	
DLG	ResNet-121	97.27%	1	25.14%	45.57%	51.86%	700
	DenseNet-18	97.11%	1	15.57%	33.57%	42.14%	700
GRNN	ResNet-121	97.27%	1	30.66%	74.79%	88.40%	700
			4	17.45%	24.64%	31.11%	1112
			8	6.14%	13.58%	22.13%	2224
			16	2.90%	10.43%	22.08%	4352
	DenseNet-18	97.11%	1	11.46%	43.12%	63.03%	700
			4	9.53%	19.87%	26.80%	1112
			8	3.06%	10.25%	19.83%	2224
			16	1.52%	8.23%	19.12%	4352

Table 9. The re-identification results from two examples of true images and their corresponding generated fake images.

ReID Result	Failure	Success
True Image		
Prediction Confidence	80.20%	91.89%
Generated Image		
Prediction Confidence	16.37%	47.30%

guaranteed in encrypted data format, which usually leads to a learning model with poor generalisation ability. Gradient encryption is an alternative defense strategy. In [24, 2, 23], the authors proposed a mechanism that uses HE to encrypt the gradient shared between server and clients, therefore, the aggregation can be done directly on the encrypted gradient. The works reported in [58, 23, 62, 68] adopted DP by adding noise to local gradient. Each trainable parameter in the learning model is given a noise bound, therefore, the computational efficiency is limited by the number of learning parameters.

The most relevant defense approach for GRNN is DP, where the clients can add a level of Gaussian or Laplacian noise onto the shared gradient. Formally, DP can be defined as such:  $Pr(f(D) = y) \leq e^\epsilon \times Pr(f(D') = y)$ , where  $D$  and  $D'$  are the raw data and the noised data, respectively.

The learning algorithm  $f$  ensures two probabilities are sufficiently close for any output  $y$ , then  $f$  is so-called  $\epsilon$ -DP. We empirically evaluated the effectiveness of GRNN when DP defense strategy was used. In this study, the *LeNet* was used as the global FL model with different batch sizes. We varied the scale of noise but fixed the  $\epsilon$ , where the  $\mu$  (mean value for Gaussian, distribution peak for Laplacian) was set to 0, and range  $\lambda$  (standard deviation for Gaussian, exponential decay for Laplacian) from 1e-1 to 1e-4. Fig. 6 shows the MSE distance between recovered image and true image when different levels and types of noise are added. GRNN fails to recover the image when a high level of noise is added to the gradient (see Figs. 6 (a) and (e)), however, this usually leads to poor performance on the global FL model as the noisy gradients are aggregated. We observe that GRNN is able to recover the image data successfully and obtain reasonable results when the scale of noise reduced to 0.01 (see Figs. 6 (b) and (f)). The PSNR scores are presented in Table 10. Compared to the no-defense approach shown in Table 5, the noise added to the gradient can result in decreasing of PSNR of the generated images, which indicates the effectiveness of DP strategy. However, the proposed GRNN is still capable of recovering image data when a high level of noise is added to the gradient, *i.e.*, 1e-2. The PSNR scores with Gaussian noise scale of 1e-4 on MNIST dataset are even larger than that without noise (52.51% VS. 52.37%), as well on LFW dataset (46.26% VS. 45.57%). On the other hand, we found that even the image recovery fails, the label can still be inferred correctly using our GRNN. However, DLG totally fails to recover images and inference labels in all of

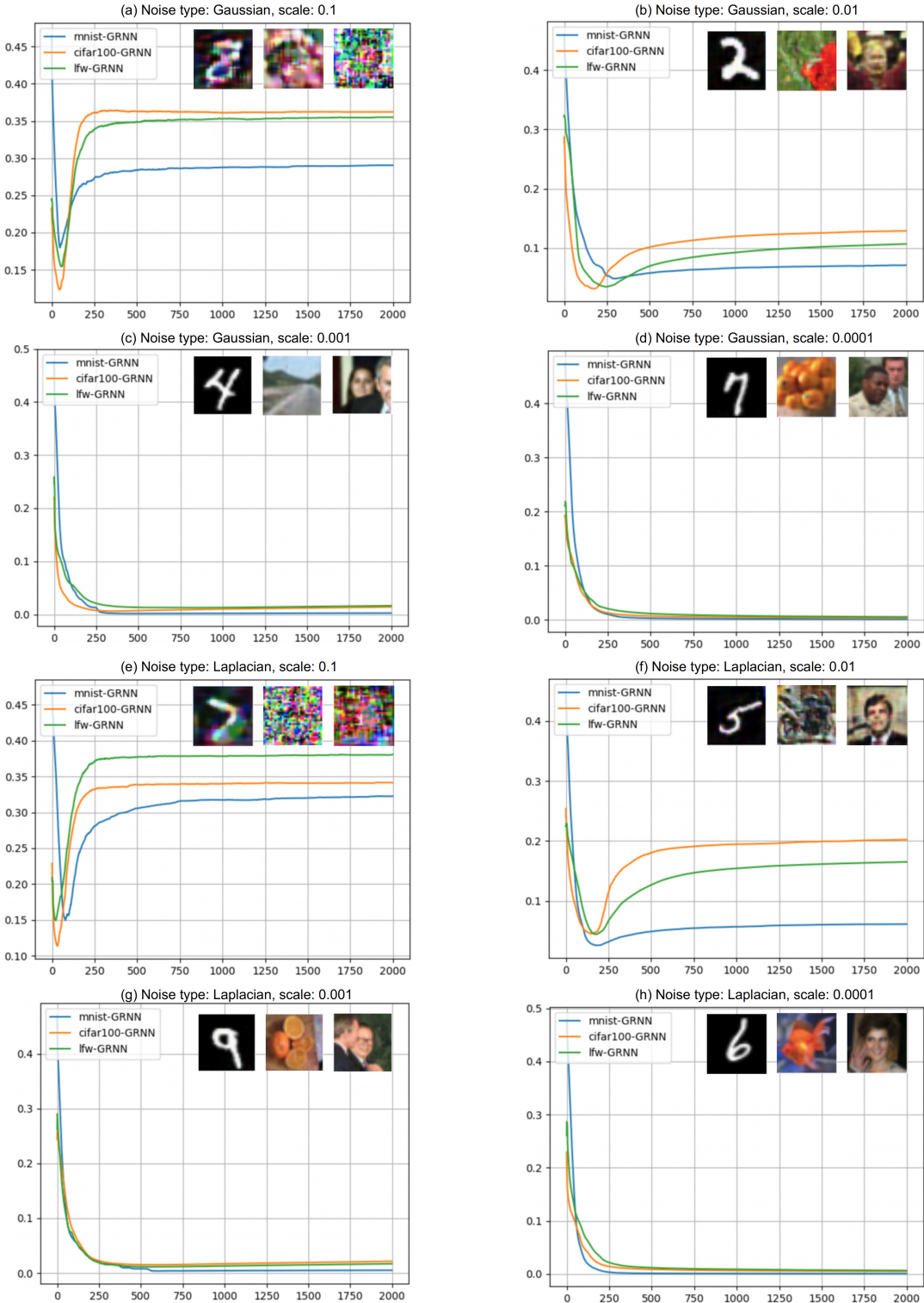


Figure 6. MSE distances between true images and generated fake images during training and illustration of generated fake images from GRNN with different noise types and scales on three datasets. (a) - (d) are the results of adding Gaussian noise, and (e) - (h) are the results of adding Laplacian noise. The horizontal axis is the number of iteration for training the attacking model.

Table 10. PSNR scores with different noise types and scales. “ $\times$ ” means the method fails the experiment, whereas PSNR score is given only if it successes. DLG failed completely, as it had no visible success among all the experiments.

Method	Dataset	Scale Type	Batch Size	1e-1	1e-2	1e-3	1e-4
DLG	MNIST	Gaussian	1	$\times$	$\times$	$\times$	$\times$
			4	$\times$	$\times$	$\times$	$\times$
		Laplacian	1	$\times$	$\times$	$\times$	$\times$
			4	$\times$	$\times$	$\times$	$\times$
	CIFAR-100	Gaussian	1	$\times$	$\times$	$\times$	$\times$
			4	$\times$	$\times$	$\times$	$\times$
		Laplacian	1	$\times$	$\times$	$\times$	$\times$
			4	$\times$	$\times$	$\times$	$\times$
Ours	MNIST	Gaussian	1	39.73	39.73	47.20	52.51
			4	$\times$	39.66	39.67	44.43
			8	$\times$	40.11	39.65	40.71
			16	$\times$	$\times$	39.73	39.78
		Laplacian	1	39.69	39.55	45.08	51.80
			4	$\times$	39.67	39.83	45.39
			8	$\times$	$\times$	39.66	41.02
			16	$\times$	$\times$	39.62	40.00
	CIFAR-100	Gaussian	1	$\times$	38.18	41.78	45.75
			4	$\times$	$\times$	38.29	40.64
			8	$\times$	$\times$	38.18	39.26
			16	$\times$	$\times$	$\times$	38.65
		Laplacian	1	$\times$	38.13	40.17	46.20
			4	$\times$	$\times$	38.14	40.32
			8	$\times$	$\times$	38.08	39.14
			16	$\times$	$\times$	$\times$	$\times$
	LFW	Gaussian	1	$\times$	38.15	41.72	46.26
			4	$\times$	$\times$	38.25	40.59
			8	$\times$	$\times$	$\times$	$\times$
			16	$\times$	$\times$	$\times$	$\times$
		Laplacian	1	$\times$	38.09	40.96	46.09
			4	$\times$	$\times$	38.19	40.26
			8	$\times$	$\times$	$\times$	$\times$
			16	$\times$	$\times$	$\times$	$\times$

our experiments.

## 5. Conclusion

In this paper, we proposed a data leakage attack method, namely GRNN, for FL system, which consists of a fake data generator and a fake label generator branches. The model is learned to approximate the shared gradient between server and clients by generating fake data that are closer to the original data. The experimental results show that GRNN is capable of recovering both data and its corresponding label. Compared to the state-of-the-art DLG, the proposed method is significantly more stable when a large batch size is used and outperforms in terms of quality of recovered data and

accuracy of label inference. Meanwhile, the experimental results on face re-identification task using generated image show that GRNN outperforms DLG significantly in terms of *Top-1*, *Top-3* and *Top-5* accuracies. In addition to the attack method, we also discussed the potential defense strategies and empirically evaluate the performance of GRNN when DP defense is applied to the shared gradient. We conclude that our method can successfully and consistently recover the data in FL when a high level of noise is added to the gradient. The implementation of our method is publicly available to ensure its reproducibility.

## References

- [1] Martin Abadi, Andy Chu, Ian Goodfellow, H Brendan McMahan, Ilya Mironov, Kunal Talwar, and Li Zhang. Deep learning with differential privacy. In *ACM CCS*, pages 308–318, 2016. 11
- [2] Yoshinori Aono, Takuya Hayashi, Lihua Wang, Shiho Moriai, et al. Privacy-preserving deep learning via additively homomorphic encryption. *IEEE Trans. on Information Forensics and Security*, 13(5):1333–1345, 2017. 12
- [3] Frederik Armknecht, Colin Boyd, Christopher Carr, Kristian Gjøsteen, Angela Jäschke, Christian A Reuter, and Martin Strand. A guide to fully homomorphic encryption. *IACR Cryptol. ePrint Arch.*, 2015:1192, 2015. 11
- [4] Louis JM Aslett, Pedro M Esperança, and Chris C Holmes. Encrypted statistical machine learning: new privacy preserving methods. *arXiv preprint arXiv:1508.06845*, 2015. 11
- [5] Giuseppe Ateniese, Luigi V Mancini, Angelo Spognardi, Antonio Villani, Domenico Vitali, and Giovanni Felici. Hacking smart machines with smarter ones: How to extract meaningful data from machine learning classifiers. *International Journal of Security and Networks*, 10(3):137–150, 2015. 2
- [6] Leonard E Baum and Ted Petrie. Statistical inference for probabilistic functions of finite state markov chains. *The annals of mathematical statistics*, 37(6):1554–1563, 1966. 2
- [7] Keith Bonawitz, Vladimir Ivanov, Ben Kreuter, Antonio Marcedone, H Brendan McMahan, Sarvar Patel, Daniel Ramage, Aaron Segal, and Karn Seth. Practical secure aggregation for federated learning on user-held data. *arXiv preprint arXiv:1611.04482*, 2016. 11
- [8] Bernhard E Boser, Isabelle M Guyon, and Vladimir N Vapnik. A training algorithm for optimal margin classifiers. In *Proceedings of the fifth annual workshop on Computational learning theory*, pages 144–152, 1992. 2
- [9] Raphael Bost, Radu Ada Popa, Stephen Tu, and Shafi Goldwasser. Machine learning classification over encrypted data. In *NDSS*, volume 4324, page 4325, 2015. 11
- [10] Zhiqi Bu, Jinshuo Dong, Qi Long, and Weijie J Su. Deep learning with gaussian differential privacy. *Harvard data science review*, 2020(23), 2020. 11
- [11] David Carrell, Bradley Malin, John Aberdeen, Samuel Bayer, Cheryl Clark, Ben Wellner, and Lynette Hirschman. Hiding in plain sight: use of realistic surrogates to reduce exposure of protected health information in clinical text. *Journal of the American Medical Informatics Association*, 20(2):342–348, 2013. 2
- [12] Di Chai, Leye Wang, Kai Chen, and Qiang Yang. Fedeval: A benchmark system with a comprehensive evaluation model for federated learning. *arXiv preprint arXiv:2011.09655*, 2020. 1
- [13] Trishul Chilimbi, Yutaka Suzue, Johnson Apacible, and Karthik Kalyanaraman. Project adam: Building an efficient and scalable deep learning training system. In *OSDI*, pages 571–582, 2014. 1
- [14] Jeffrey Dean, Greg S Corrado, Rajat Monga, Kai Chen, Matthieu Devin, Quoc V Le, Mark Z Mao, Marc’Aurelio Ranzato, Andrew Senior, Paul Tucker, et al. Large scale distributed deep networks. 2012. 1
- [15] Cynthia Dwork, Aaron Roth, et al. The algorithmic foundations of differential privacy. *Foundations and Trends in Theoretical Computer Science*, 9(3-4):211–407, 2014. 11
- [16] Matt Fredrikson, Somesh Jha, and Thomas Ristenpart. Model inversion attacks that exploit confidence information and basic countermeasures. In *ACM CCS*, pages 1322–1333, 2015. 1, 3
- [17] Matthew Fredrikson, Eric Lantz, Somesh Jha, Simon Lin, David Page, and Thomas Ristenpart. Privacy in pharmacogenetics: An end-to-end case study of personalized warfarin dosing. In *USENIX*, pages 17–32, 2014. 3
- [18] Adrià Gascón, Philipp Schoppmann, Borja Balle, Mariana Raykova, Jack Doerner, Samee Zahur, and David Evans. Secure linear regression on vertically partitioned datasets. *IACR Cryptol. ePrint Arch.*, 2016:892, 2016. 11
- [19] Robin C Geyer, Tassilo Klein, and Moin Nabi. Differentially private federated learning: A client level perspective. *arXiv preprint arXiv:1712.07557*, 2017. 1
- [20] Ran Gilad-Bachrach, Nathan Dowlin, Kim Laine, Kristin Lauter, Michael Naehrig, and John Wernsing. Cryptonets: Applying neural networks to encrypted data with high throughput and accuracy. In *ICML*, pages 201–210. PMLR, 2016. 11
- [21] Gene H Golub and James M Ortega. *Scientific computing: an introduction with parallel computing*. Elsevier, 2014. 1
- [22] Ian Goodfellow, Jean Pouget-Abadie, Mehdi Mirza, Bing Xu, David Warde-Farley, Sherjil Ozair, Aaron Courville, and Yoshua Bengio. Generative adversarial nets. In *NIPS*, pages 2672–2680, 2014. 1
- [23] Meng Hao, Hongwei Li, Guowen Xu, Sen Liu, and Haomiao Yang. Towards efficient and privacy-preserving federated deep learning. In *ICC*, pages 1–6. IEEE, 2019. 12
- [24] Stephen Hardy, Wilko Henecka, Hamish Ivey-Law, Richard Nock, Giorgio Patrini, Guillaume Smith, and Brian Thorne. Private federated learning on vertically partitioned data via entity resolution and additively homomorphic encryption. *arXiv preprint arXiv:1711.10677*, 2017. 12
- [25] Kaiming He, Xiangyu Zhang, Shaoqing Ren, and Jian Sun. Deep residual learning for image recognition. In *CVPR*, pages 770–778, 2016. 1, 6
- [26] Ehsan Hesamifard, Hassan Takabi, and Mehdi Ghasemi. Cryptodl: Deep neural networks over encrypted data. *arXiv preprint arXiv:1711.05189*, 2017. 11
- [27] Ehsan Hesamifard, Hassan Takabi, and Mehdi Ghasemi. Deep neural networks classification over encrypted data. In *ACM CODASYL*, pages 97–108, 2019. 11
- [28] Briland Hitaj, Giuseppe Ateniese, and Fernando Perez-Cruz. Deep models under the gan: information leakage from collaborative deep learning. In *ACM CCS*, pages 603–618, 2017. 1, 3
- [29] Alain Hore and Djemel Ziou. Image quality metrics: Psnr vs. ssim. In *2010 20th international conference on pattern recognition*, pages 2366–2369. IEEE, 2010. 6
- [30] Gary B Huang, Marwan Mattar, Tamara Berg, and Eric Learned-Miller. Labeled faces in the wild: A database for studying face recognition in unconstrained environments. 2008. 6
- [31] Forrest N Iandola, Matthew W Moskewicz, Khalid Ashraf, and Kurt Keutzer. Firecaffe: near-linear acceleration of deep

- neural network training on compute clusters. In *CVPR*, pages 2592–2600, 2016. 1
- [32] Alex Krizhevsky, Geoffrey Hinton, et al. Learning multiple layers of features from tiny images. 2009. 6
- [33] Alex Krizhevsky, Ilya Sutskever, and Geoffrey E Hinton. Imagenet classification with deep convolutional neural networks. *Communications of the ACM*, 60(6):84–90, 2017. 1
- [34] Owusu-Agyemang Kwabena, Zhen Qin, Tianming Zhuang, and Zhiguang Qin. Mscryptonet: Multi-scheme privacy-preserving deep learning in cloud computing. *IEEE Access*, 7:29344–29354, 2019. 11
- [35] Martha Larson, Zhuoran Liu, SFB Brugman, and Zhengyu Zhao. Pixel privacy: increasing image appeal while blocking automatic inference of sensitive scene information. 2018. 10
- [36] Yann LeCun. The mnist database of handwritten digits. <http://yann.lecun.com/exdb/mnist/>, 1998. 6
- [37] Yann LeCun, Yoshua Bengio, and Geoffrey Hinton. Deep learning. *nature*, 521(7553):436–444, 2015. 1
- [38] Yann LeCun, Léon Bottou, Yoshua Bengio, and Patrick Haffner. Gradient-based learning applied to document recognition. *Proceedings of the IEEE*, 86(11):2278–2324, 1998. 6
- [39] Fenghua Li, Zhe Sun, Ang Li, Ben Niu, Hui Li, and Guohong Cao. Hideme: Privacy-preserving photo sharing on social networks. In *INFOCOM*, pages 154–162. IEEE, 2019. 2
- [40] Mu Li, David G Andersen, Jun Woo Park, Alexander J Smola, Amir Ahmed, Vanja Josifovski, James Long, Eugene J Shekita, and Bor-Yiing Su. Scaling distributed machine learning with the parameter server. In *OSDI*, pages 583–598, 2014. 1
- [41] Yujun Lin, Song Han, Huiyi Mao, Yu Wang, and William J Dally. Deep gradient compression: Reducing the communication bandwidth for distributed training. *arXiv preprint arXiv:1712.01887*, 2017. 1
- [42] Brendan McMahan, Eider Moore, Daniel Ramage, Seth Hampson, and Blaise Aguera y Arcas. Communication-efficient learning of deep networks from decentralized data. In *AISTATS*, pages 1273–1282. PMLR, 2017. 1, 3
- [43] Richard McPherson, Reza Shokri, and Vitaly Shmatikov. Defeating image obfuscation with deep learning. *arXiv preprint arXiv:1609.00408*, 2016. 2
- [44] Luca Melis, Congzheng Song, Emiliano De Cristofaro, and Vitaly Shmatikov. Exploiting unintended feature leakage in collaborative learning. In *IEEE SP*, pages 691–706. IEEE, 2019. 1, 3
- [45] Apostolos Modas, Seyed-Mohsen Moosavi-Dezfooli, and Pascal Frossard. Sparsefool: a few pixels make a big difference. In *CVPR*, pages 9087–9096, 2019. 10
- [46] Payman Mohassel and Yupeng Zhang. Secureml: A system for scalable privacy-preserving machine learning. In *IEEE SP*, pages 19–38. IEEE, 2017. 11
- [47] Seyed-Mohsen Moosavi-Dezfooli, Alhussein Fawzi, and Pascal Frossard. Deepfool: a simple and accurate method to fool deep neural networks. In *CVPR*, pages 2574–2582, 2016. 10
- [48] Philipp Moritz, Robert Nishihara, Ion Stoica, and Michael I Jordan. Sparknet: Training deep networks in spark. *arXiv preprint arXiv:1511.06051*, 2015. 1
- [49] Karthik Nandakumar, Nalini Ratha, Sharath Pankanti, and Shai Halevi. Towards deep neural network training on encrypted data. In *CVPR*, pages 0–0, 2019. 11
- [50] Valeria Nikolaenko, Udi Weinsberg, Stratis Ioannidis, Marc Joye, Dan Boneh, and Nina Taft. Privacy-preserving ridge regression on hundreds of millions of records. In *IEEE SP*, pages 334–348. IEEE, 2013. 11
- [51] Nicolas Papernot, Patrick McDaniel, Somesh Jha, Matt Fredrikson, Z Berkay Celik, and Ananthram Swami. The limitations of deep learning in adversarial settings. In *IEEE EuroS&P*, pages 372–387. IEEE, 2016. 10
- [52] Omkar M Parkhi, Andrea Vedaldi, and Andrew Zisserman. Deep face recognition. 2015. 6
- [53] Adam Paszke, Sam Gross, Soumith Chintala, Gregory Chanan, Edward Yang, Zachary DeVito, Zeming Lin, Alban Desmaison, Luca Antiga, and Adam Lerer. Automatic differentiation in pytorch. 2017. 6
- [54] Pitch Patarasuk and Xin Yuan. Bandwidth optimal all-reduce algorithms for clusters of workstations. *Journal of Parallel and Distributed Computing*, 69(2):117–124, 2009. 1
- [55] NhatHai Phan, Xintao Wu, Han Hu, and Dejing Dou. Adaptive laplace mechanism: Differential privacy preservation in deep learning. In *ICDM*, pages 385–394. IEEE, 2017. 11
- [56] Leonid I Rudin, Stanley Osher, and Emad Fatemi. Nonlinear total variation based noise removal algorithms. *Physica D: nonlinear phenomena*, 60(1-4):259–268, 1992. 5
- [57] Ali Shahin Shamsabadi, Ricardo Sanchez-Matilla, and Andrea Cavallaro. Colorfool: Semantic adversarial colorization. In *CVPR*, pages 1151–1160, 2020. 10
- [58] Reza Shokri and Vitaly Shmatikov. Privacy-preserving deep learning. In *ACM CCS*, pages 1310–1321, 2015. 3, 12
- [59] Reza Shokri, Marco Stronati, Congzheng Song, and Vitaly Shmatikov. Membership inference attacks against machine learning models. In *IEEE SP*, pages 3–18. IEEE, 2017. 1, 2
- [60] Alysa Ziying Tan, Han Yu, Lizhen Cui, and Qiang Yang. Towards personalized federated learning. *arXiv preprint arXiv:2103.00710*, 2021. 1
- [61] Eric P Xing, Qirong Ho, Wei Dai, Jin Kyu Kim, Jinliang Wei, Seunghak Lee, Xun Zheng, Pengtao Xie, Abhimanu Kumar, and Yaoliang Yu. Petuum: A new platform for distributed machine learning on big data. *IEEE Trans. on Big Data*, 1(2):49–67, 2015. 1
- [62] Chugui Xu, Ju Ren, Deyu Zhang, Yaoxue Zhang, Zhan Qin, and Kui Ren. Ganofuscator: Mitigating information leakage under gan via differential privacy. *IEEE Trans. on Information Forensics and Security*, 14(9):2358–2371, 2019. 12
- [63] Qiang Yang, Yang Liu, Yong Cheng, Yan Kang, Tianjian Chen, and Han Yu. Federated learning. *Synthesis Lectures on Artificial Intelligence and Machine Learning*, 13(3):1–207, 2019. 1
- [64] Matthew D Zeiler, Dilip Krishnan, Graham W Taylor, and Rob Fergus. Deconvolutional networks. In *CVPR*, pages 2528–2535. IEEE, 2010. 4
- [65] Matthew D Zeiler, Graham W Taylor, and Rob Fergus. Adaptive deconvolutional networks for mid and high level feature learning. In *ICCV*, pages 2018–2025. IEEE, 2011. 4

- [66] Yuheng Zhang, Ruoxi Jia, Hengzhi Pei, Wenxiao Wang, Bo Li, and Dawn Song. The secret revealer: Generative model-inversion attacks against deep neural networks. In *CVPR*, pages 253–261, 2020. [2](#)
- [67] Bo Zhao, Konda Reddy Mopuri, and Hakan Bilen. idlg: Improved deep leakage from gradients. *arXiv preprint arXiv:2001.02610*, 2020. [1, 3](#)
- [68] Jingwen Zhao, Yunfang Chen, and Wei Zhang. Differential privacy preservation in deep learning: Challenges, opportunities and solutions. *IEEE Access*, 7:48901–48911, 2019. [12](#)
- [69] Ligeng Zhu, Zhijian Liu, and Song Han. Deep leakage from gradients. In *NIPS*, pages 14774–14784, 2019. [1, 3](#)
- [70] Martin Zinkevich, Markus Weimer, Alexander J Smola, and Lihong Li. Parallelized stochastic gradient descent. In *NIPS*, volume 4, page 4. Citeseer, 2010. [1](#)